

**Volume 50 (2017)**

**Supporting information for article:**

**Whole-nanoparticle atomistic modelling of the schwertmannite structure from total scattering data**

**M. Sestu, G. Navarra, S. Carrero, S. M. Valvidares, G. Aquilanti, R. Pérez-Lopez and A. Fernandez-Martinez**

### S1. RMC-DSE refinement code

In order to study the structure of schwertmannite a specific routine (RMC-DSE) for the refinement of nanoparticles was built. In this routine a starting model was refined by applying an algorithm similar to Reverse Monte Carlo (RMC) [1]. As commonly done in the RMC approach, small atomic displacements were randomly applied simulating the thermal and the surface relaxation disorders. The displacements were accepted or rejected on the basis of the agreement between experimental and calculated structural functions. Structure Factor and their Fourier Transform related Pair Distribution Function (PDF) were simultaneously used in the optimization procedure.

To speed up the calculation the most time-consuming part of the code was allowed to run on a fast graphics processing unit (GPU). The whole (RMC-DSE) routine was written in C/C++/CUDA [2].

The Structure Factor  $S(Q)$  of the starting model was calculated through the Debye Scattering Equation (DSE)  $I_{coh}(Q)$ , which represents the coherent scattering contribution to the X-ray diffraction powder pattern:

$$I_{coh}(Q) = \frac{1}{N} \sum_{i=1}^N \sum_{j=1}^N f_i(Q) f_j(Q) \frac{\sin(Qr_{ij})}{Qr_{ij}}$$

$$Q = 4\pi \sin(\theta/\lambda)$$

where  $q$  is the scattering vector being  $\theta$  the half scattering angle and  $\lambda$  the wavelength of the incident radiation;  $N$  is the total number of atoms;  $f_i(Q)$  is the atomic scattering factor of the  $i$ -th atom and  $r_{ij}$  is the distance between the atoms  $i$  and  $j$ .

$$S(Q) = \frac{I_{coh}(Q) - \langle f(Q)^2 \rangle}{\langle f(Q)^2 \rangle} + 1$$

$$\langle f(Q)^2 \rangle = \sum_{m=1}^M x_m f_m(Q)^2$$

$$\langle f(Q) \rangle^2 = \left( \sum_{m=1}^M x_m f_m(Q) \right)^2$$

where  $x_m$  is the molar fraction of the element  $m$ ,  $f_m$  is the atomic form factor of the element  $m$  and  $M$  is the number of atomic species.

The PDF function is calculated applying the Fourier Transform to the  $S(Q)$ , which is damped at  $Q_{\max}$  by the Hann Function:

The calculated functions were compared with the corresponding experimental functions using the  $\chi^2$  parameter:

$$\chi^2 = \frac{W_S}{\sigma^2} \frac{\sum^{NQ} (S_{\text{exp}}(Q) - S_{\text{calc}}(Q))^2}{NQ} + \frac{W_{PDF}}{\sigma^2} \frac{\sum^{NR} (PDF_{\text{exp}}(r) - PDF_{\text{calc}}(r))^2}{NR}$$

where  $W_S$  and  $W_{PDF}$  can balance the weight of the each contribution,  $\sigma$  is called the temperature factor,  $NQ$  and  $NR$  are the number of points of the  $S(Q)$  and PDF functions. The temperature factor can be tuned to allow a smaller or a greater number of moves in order to avoid local minimum traps.

The optimization procedure can be summarized as follows:

- One atom is randomly chosen and its coordinates are randomly modified within a maximum displacement value. The new coordinates should satisfy constraints over the minimum and the maximum distance allowed between neighboring atoms. A new atomic configuration is then obtained.
- New  $S(Q)$  and their Fourier Transform are calculated.
- In order to reduce the computation time the new  $S(Q)$  is calculated as follows:

$$S'(Q) = S(Q) - \frac{2}{N} \sum_j f_k f_j \frac{\sin(Qr_{kj})}{Qr_{kj}} + \frac{2}{N} \sum_j f_k f_j \frac{\sin(Qr'_{kj})}{Qr'_{kj}}$$

where  $k$  is the moved atom,  $r_{kj}$  and  $r'_{kj}$  are the distances between atoms  $k$  and  $j$  before and after the move, respectively. In this way, only the contributions of the moved atom with the others are taken into account. Furthermore, the two contributions are simultaneously calculated through parallel computing using an Nvidia GeForce gtx 690 GPU.

The Fourier Transform of the  $S'(Q)$  provides a new PDF' and a new  $\chi'^2$  is calculated. If the new value of the agreement parameter is less than the old value the move is accepted. If not the move could be accepted according with the conditional probability :

$$rnd[0; 1] \leq e^{-(\chi'^2 - \chi^2)/2}$$

The smaller the difference between  $\chi'^2$  and  $\chi^2$ , the higher the probability.

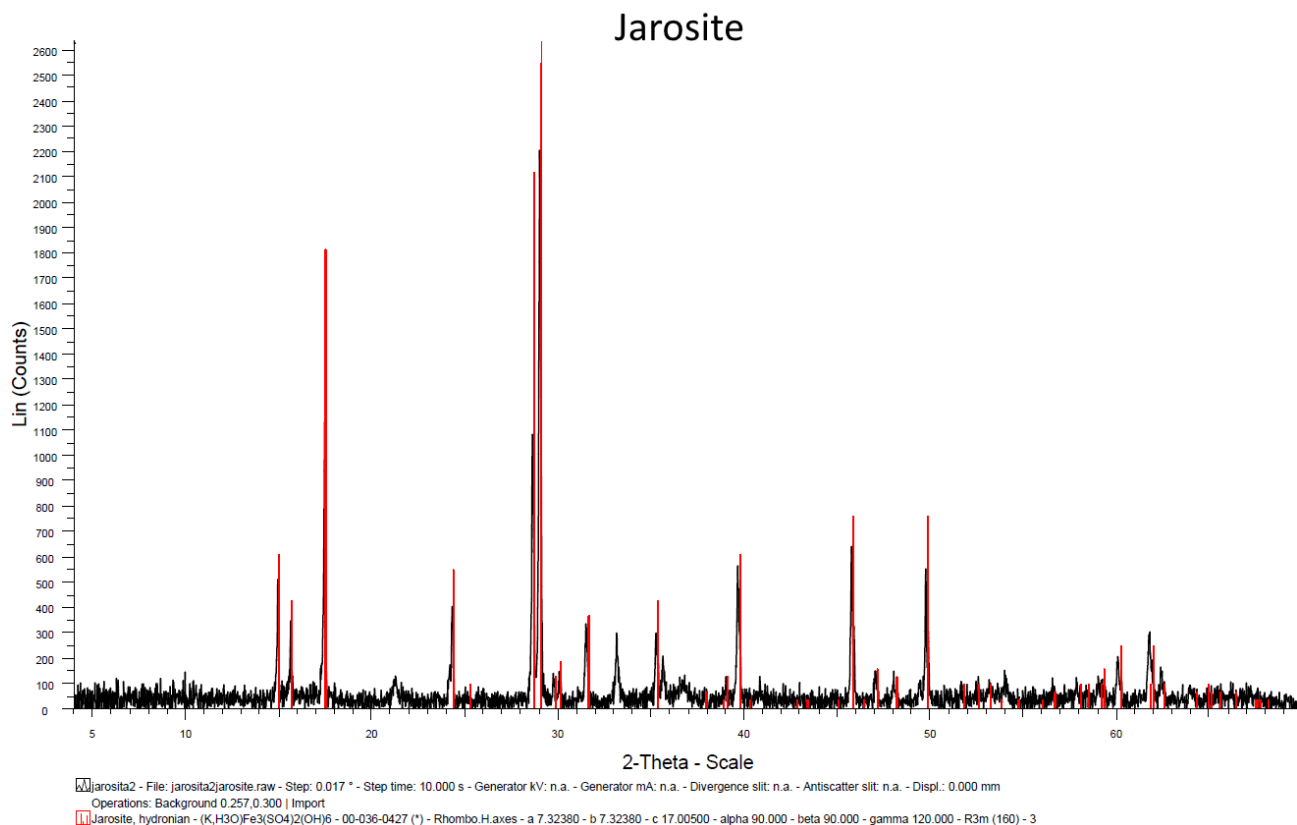
- Another atom is then randomly chosen and moved and the recursive procedure continues until convergence.

## References

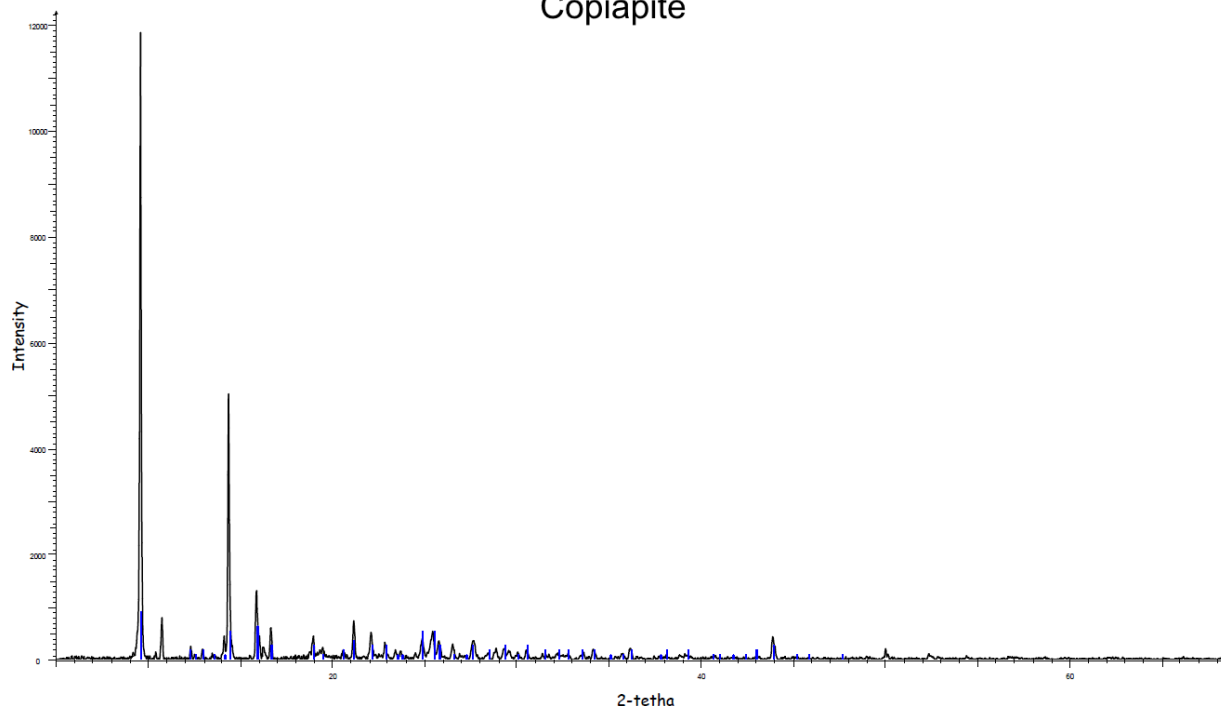
- [1] McGreevy R.L. and Pusztai L., Molecular Simulation, 1, 359-367, 1988.
- [2] Cuda Programming Guide 2.3 Nvidia Corp.

## X-ray diffraction characterization of halotrichite and copiapite samples

The experimental diffraction patterns of jarosite, copiapite and halotrichite samples are shown in Figure S1, together with the reflections for each phase, from PDF files #00-036-0427 (jarosite), #00-039-1387 (halotrichite) and #00-035-0583 (copiapite). A small level of impurities (not identified) has been found in the halotrichite sample. These does not seem to affect the results of the S-XANES analyses, with the halotrichite sample not showing any pre-peak, as expected.

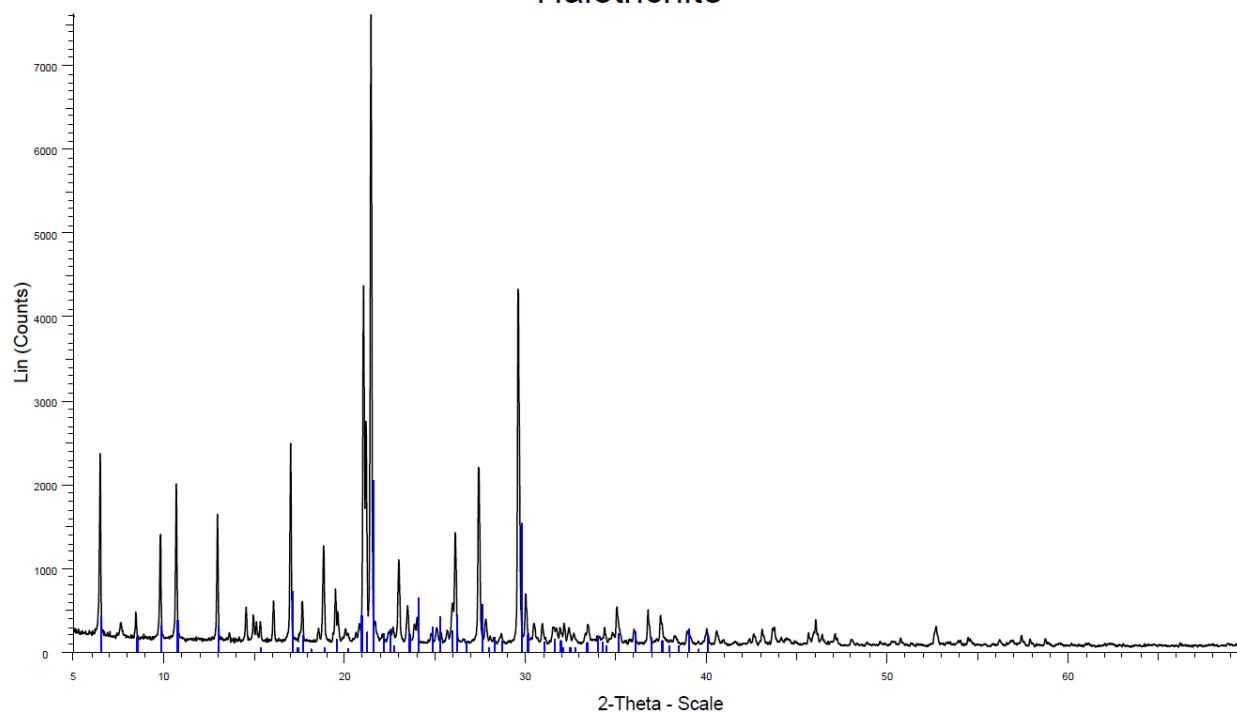


### Copiapite



File: copiapite.raw - Step: 0.026 ° - Step time: 6.000 s - Anode: Cu - Generator kV: 40 kV - Generator mA: 40 mA - Divergence slit: 0.298 ° - Antiscatter slit: 0.298 ° - Displ.: 0.000 mm  
 Copiapite - FeFe4(SO4)6(OH)2·20H2O - 00-035-0583 (I) - Triclinic - a 7.33700 - b 18.76000 - c 7.37900 - alpha 91.460 - beta 102.180 - gamma 98.950 - P-1 (2) - 1

### Halotrichite



Halotrichite - File: Halotrichite.raw - Step: 0.026 ° - Step time: 7.000 s - Anode: Co - Generator kV: 40 kV - Generator mA: 39 mA - Divergence slit: n.a. - Antiscatter slit: n.a. - Displ.: 0.000 mm  
 Operations: Import  
 Halotrichite - Fe+2Al2(SO4)4·22H2O - 00-039-1387 (I) - Monoclinic - a 6.19540 - b 24.26200 - c 21.26200 - alpha 90.000 - beta 100.300 - gamma 90.000 - P21/c (14) - 4

## Schwertmannite S EXAFS

	Fit	Coordination	Proporti	$\chi^2$	R-	Ind.	Varia	Ind.	Red.	Model	Model	F-	Proba
	1	1	on (%)		factor	Point	ble	Variable	$\chi^2$	1	2	test	bility
													(%)
Sch-Nat	1	b. b. inner sp.	100	11.50	0.007	9.79	6	3.79	3.06	Fit 1	Fit 2	1.62	72.00
	2	b. b. inner sp.	50	21.36	0.013	9.79	4	5.79	3.69	Fit 1	Fit 3	1.26	64.00
	3	outer sp.	100	26.78	0.016	9.79	2	7.79	3.44				
Sch-Syn	1	b. b. inner sp.	75	20.76	0.008	13.10	7	6.10	3.40	Fit 1	Fit 2	43.85	99.99
	2	b. b. inner sp.	50	27.75	0.011	10.15	4	6.15	4.51	Fit 1	Fit3	2.05	83.00
	3	outer sp.	100	35.02	0.008	10.15	2	8.15	4.30				

b. b. inner sp.: bidentate binucleate inner-sphere

outer sp.: outer-sphere

**Table S1.** Results of the F-tests performed using different hypotheses. Only the inclusion of the fit2 (with two shells) yields a probability of statistical significance higher than 90%.

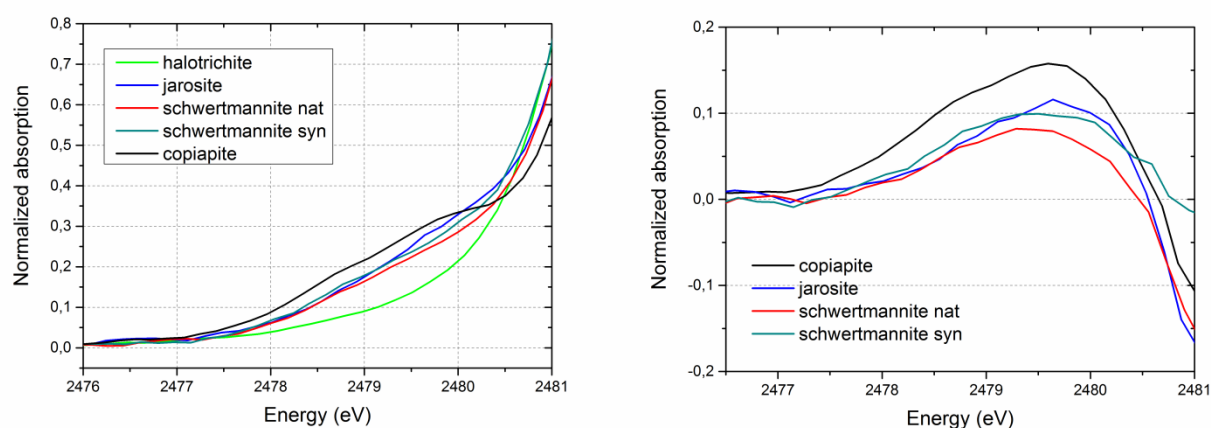


**Figure S2.** Left: Detail of the pre-edge region of the normalized X-ray absorption spectroscopy spectra of schwertmannite and the references. Right: Difference normalized spectra using the spectrum of halotrichite (free sulfate) as reference.

**Rietveld refinement***Goethite starting model CIF file*

data\_global

\_chemical\_name\_mineral 'Goethite'

loop\_

\_publ\_author\_name

'Gualtieri A'

'Venturelli P'

\_journal\_name\_full 'American Mineralogist'

\_journal\_volume 84

\_journal\_year 1999

\_journal\_page\_first 895

\_journal\_page\_last 904

\_publ\_section\_title

;

In situ study of the goethite-hematite phase transformation by real time  
synchrotron powder diffraction

Sample at T = 25 C

;

\_database\_code\_amcsd 0002226

\_chemical\_formula\_sum 'Fe H O2'

\_cell\_length\_a 9.9134

\_cell\_length\_b 3.0128

\_cell\_length\_c 4.5800

\_cell\_angle\_alpha 90

\_cell\_angle\_beta 90

\_cell\_angle\_gamma 90

\_cell\_volume 136.791

\_exptl\_crystal\_density\_diffn 4.314

\_symmetry\_space\_group\_name\_H-M 'P n m a'

loop\_

\_space\_group\_symop\_operation\_xyz

'x,y,z'

'x,1/2-y,z'

'-x,1/2+y,-z'

'1/2-x,1/2+y,1/2+z'

'1/2+x,1/2-y,1/2-z'

'1/2+x,y,1/2-z'

'1/2-x,-y,1/2+z'

'-x,-y,-z'

loop\_

\_atom\_site\_label



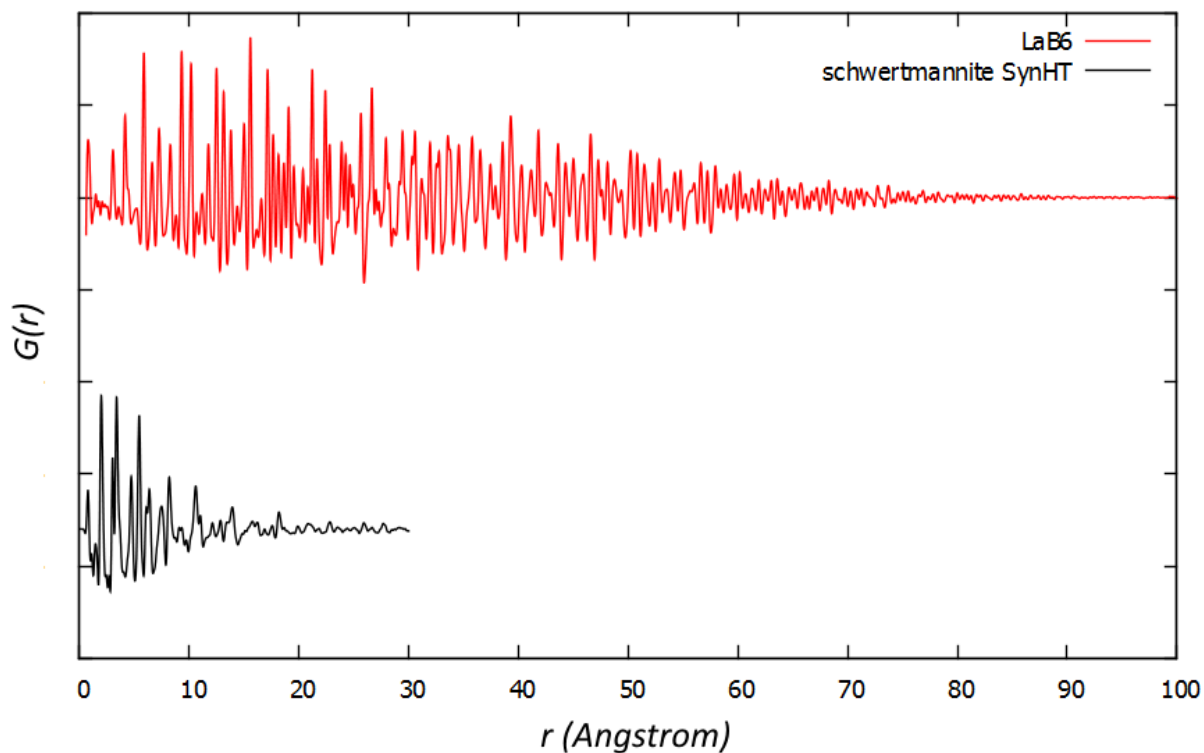
\_atom\_site\_fract\_x  
\_atom\_site\_fract\_y  
\_atom\_site\_fract\_z  
\_atom\_site\_U\_iso\_or\_equiv  
Fe 0.14590 0.25000 -0.04860 0.04900  
H -0.10100 0.25000 -0.39900 0.06000  
O1 -0.19900 0.25000 0.28500 0.04600  
O2 -0.05170 0.25000 -0.19600 0.04600

*Schwertmannite starting model CIF file*

data\_global  
\_chemical\_name\_mineral 'Schwertmannite'  
loop\_  
\_publ\_author\_name  
'Fernandez-Martinez A'  
'Timon V'  
'Roman-Ross G'  
'Cuello G J'  
'Daniels J E'  
'Ayora C'  
\_journal\_name\_full 'American Mineralogist'  
\_journal\_volume 95  
\_journal\_year 2010  
\_journal\_page\_first 1312  
\_journal\_page\_last 1322  
\_publ\_section\_title  
;  
The structure of schwertmannite, a nanocrystalline iron oxyhydroxysulfate  
Note: Model 1, positions of sulfate groups not determined  
;  
\_database\_code\_amcsd 0018670  
\_chemical\_compound\_source 'Monte Romero mine (Iberian Pyrite Belt), Spain'  
\_chemical\_formula\_sum 'Fe O2'  
\_cell\_length\_a 10.821  
\_cell\_length\_b 6.002  
\_cell\_length\_c 10.514  
\_cell\_angle\_alpha 90.0  
\_cell\_angle\_beta 92.6  
\_cell\_angle\_gamma 90.0  
\_cell\_volume 682.157  
\_exptl\_crystal\_density\_diffn 3.421  
\_symmetry\_space\_group\_name\_H-M 'P 1'

```
loop_  
_space_group_symop_operation_xyz  
'x,y,z'  
loop_  
_atom_site_label  
_atom_site_fract_x  
_atom_site_fract_y  
_atom_site_fract_z  
_atom_site_U_iso_or_equiv  
Fe 0.34500 0.00000 0.15200 0.00200  
Fe 0.14000 0.00000 0.64500 0.00200  
O 0.28800 0.00000 0.32200 0.00900  
O 0.04300 0.00000 0.33600 0.00900  
O 0.33500 0.00000 0.69000 0.00900  
O 0.32500 0.00000 0.94600 0.00900  
Fe 0.85700 0.25000 0.61100 0.00200  
Fe 0.70000 0.25000 0.09300 0.00200  
O 0.78700 0.25000 0.79600 0.00900  
O 0.54000 0.25000 0.81000 0.00900  
O 0.86100 0.25000 0.15900 0.00900  
O 0.82400 0.25000 0.41900 0.00900  
Fe 0.66900 0.00000 0.81100 0.00200  
Fe 0.86600 0.00000 0.32000 0.00200  
O 0.71100 0.00000 0.62600 0.00900  
O 0.95600 0.00000 0.61200 0.00900  
O 0.66400 0.00000 0.26000 0.00900  
O 0.67400 0.00000 0.00200 0.00900  
Fe 0.15100 0.25000 0.35200 0.00200  
Fe 0.34400 0.25000 0.84000 0.00200  
O 0.21100 0.25000 0.15200 0.00900  
O 0.45600 0.25000 0.13800 0.00900  
O 0.16500 0.25000 0.78600 0.00900  
O 0.17500 0.25000 0.52700 0.00900  
Fe 0.33700 0.50000 0.14200 0.00200  
Fe 0.14400 0.50000 0.64800 0.00200  
O 0.28800 0.50000 0.32200 0.00900  
O 0.04300 0.50000 0.33600 0.00900  
O 0.33500 0.50000 0.69000 0.00900  
O 0.32500 0.50000 0.94600 0.00900  
Fe 0.84600 0.75000 0.60600 0.00200  
Fe 0.69600 0.75000 0.09500 0.00200  
O 0.78700 0.75000 0.79600 0.00900
```

O	0.54200	0.75000	0.81000	0.00900
O	0.85700	0.75000	0.15700	0.00900
O	0.82400	0.75000	0.41900	0.00900
Fe	0.66600	0.50000	0.80400	0.00200
Fe	0.86500	0.50000	0.32200	0.00200
O	0.71100	0.50000	0.62600	0.00900
O	0.95600	0.50000	0.61200	0.00900
O	0.66400	0.50000	0.26000	0.00900
O	0.67400	0.50000	0.00200	0.00900
Fe	0.15300	0.75000	0.33800	0.00200
Fe	0.36300	0.75000	0.83500	0.00200
O	0.21100	0.75000	0.15000	0.00900
O	0.45600	0.75000	0.13800	0.00900
O	0.16500	0.75000	0.78600	0.00900
O	0.17500	0.75000	0.52800	0.00900

**RMC-DSE refinement**

**Figure S3.** Pair distribution functions of a crystalline standard (LaB<sub>6</sub>) and of schwertmannite. The dampening of the LaB<sub>6</sub> PDF is purely due to instrumental resolution effects. For schwertmannite, the dampening is dominated by the microstructure. This effect of an exponential decay in the real-space is translated into peak width in the reciprocal space.

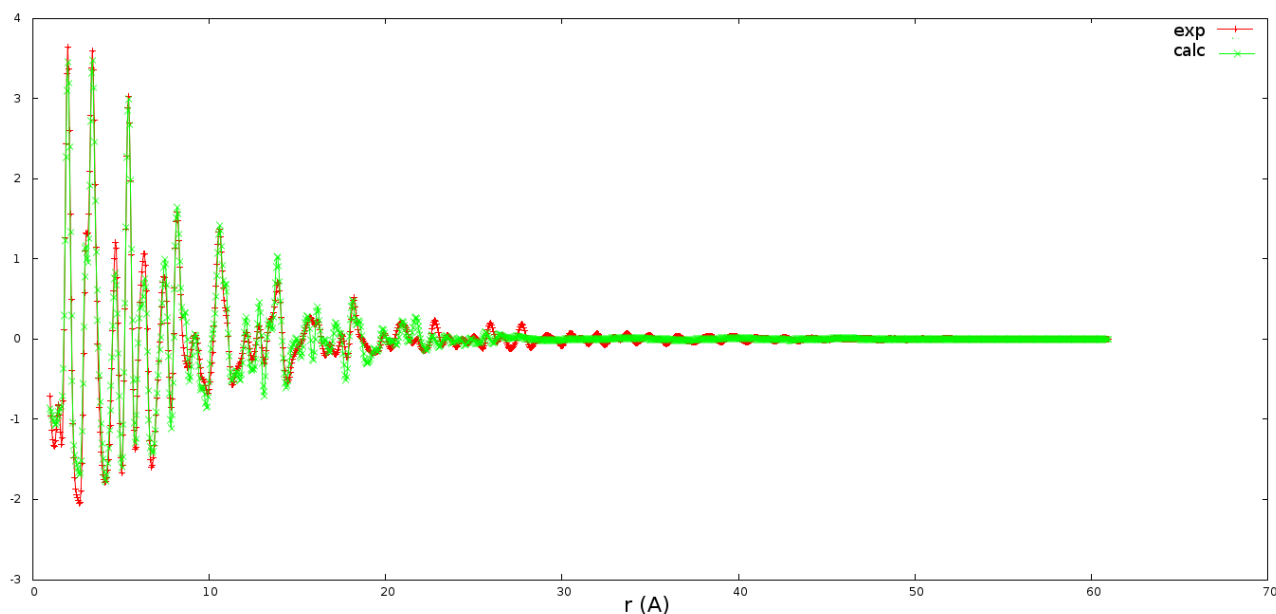


**Figure S4.** Full experimental and calculated PDFs for the sample SynHT contemplating the presence of goethite so as to appreciate the whole nanoparticle size effect.